

Spontaneous Formation of Nanoparticle Vesicles from Homopolymer Polyelectrolytes

Jennifer N. Cha,^{*,†,§} Henrik Birkedal,[†] Larken E. Euliss,[†] Michael H. Bartl,[†]
Michael S. Wong,^{†,||} Timothy J. Deming,^{†,‡} and Galen D. Stucky^{*,†,‡}

Contribution from the Department of Chemistry and Biochemistry and the Materials Department, University of California, Santa Barbara, California 93106

Received July 31, 2002; Revised Manuscript Received April 15, 2003; E-mail: j_cha@uclink.berkeley.edu; stucky@chem.ucsb.edu

Abstract: Nanoparticle vesicles were spontaneously assembled from homopolymer polyamine polyelectrolytes and water-soluble, citrate-stabilized quantum dots. The further addition of silica nanoparticles to a solution of quantum dot vesicles generated stable micrometer-sized hollow spheres whose walls were formed of a thick, inner layer of close-packed quantum dots followed by an outer layer of silica. The method employed here to assemble both the nanoparticle vesicles and the hollow spheres is in direct contrast to previous syntheses that use either tailored block copolymers or oil-in-water emulsion templating. We propose that the formation of charge-stabilized hydrogen bonds between the positively charged amines of the homopolymer polyelectrolytes and the negatively charged citrate molecules stabilizing the quantum dots is responsible for the macroscopic phase separation in this completely aqueous system. The ease and processibility of the present approach gives promise for the production of a diverse array of materials ranging in applications from drug delivery to catalysis to micrometer-scale optical devices.

Introduction

The synthesis of stable organic micelles, vesicles, and inorganic hollow spheres has garnered much interest for a variety of applications ranging from drug delivery and chemical storage and transport to waste removal. Organic micelles and vesicles are typically constructed from surfactants and block copolymers where the intrinsic differences in chemical potentials of the hydrophobic/hydrophilic regions of the surfactant or polymer blocks guide the organization of the organic groups and the interface between the solvent medium and the final structure.^{1–5} Recently, block copolypeptides have also been used to create stable and responsive vesicles that can be used for both transport and delivery.²

Three-dimensional, macroscopically phase separated inorganic systems, such as nanoparticle vesicles and hollow spheres, have been produced by using either a layer-by-layer (LBL) assembly on sacrificial templates or surfactant-stabilized oil-in-water emulsion droplets.^{6,7} For example, using the latter approach, it

is possible to synthesize hollow inorganic capsules formed of large colloidal particles (termed colloidosomes).⁸ We present here a spontaneous, one-step synthesis of cadmium selenide (CdSe) quantum dot (QD) vesicles using a combination of positively charged homopolymers and negatively charged semiconductor nanocrystals. Our QD vesicle assembly was accomplished in a completely aqueous system and with single block polyelectrolyte homopolymers. We have previously succeeded in creating multicompositional inorganic hollow spheres through self-assembly by using specifically tailored block copolypeptides.⁹ However, the cooperative assembly of inorganic nanoparticles into vesicles or hollow spheres from homopolymer polyelectrolytes is unprecedented. In contrast to earlier work, the highly structured macroscopic phase separation is driven by neither the polymers nor a previously introduced separate phase (e.g., oil-in-water emulsion or preformed polystyrene sphere) but instead by the molecular interactions between the ligands on the inorganic phase and functional groups of the organic polyelectrolyte. The spontaneous formation of these hollow entities is proposed to occur through the formation of charge-stabilized hydrogen bonding between the positively charged amines of the polyelectrolyte and the negatively charged stabilizing agents capping the QDs.

[†] Department of Chemistry and Biochemistry.

[‡] Materials Department.

[§] Current address: Department of Chemistry, D83 Hildebrand Hall, University of California, Berkeley, Berkeley, CA 94720.

^{||} Current address: Department of Chemical Engineering, Rice University, Houston, TX 77251-1892.

- (1) Zasadzinski, J. A.; Kisak, E.; Evans, C. *Curr. Opin. Colloid Interface Sci.* **2001**, *6*, 85–90.
- (2) Chécot, F.; Lecommandoux, S.; Gnanou, Y.; Klok, H.-A. *Angew. Chem., Int. Ed.* **2002**, *41*, 1339–1343.
- (3) Discher, B. M.; Won, Y. Y.; Ege, D. S.; Lee, J. C.; Bates, F. S.; Discher, D. E.; Hammer, D. A. *Science* **1999**, *284*, 1143–1146.
- (4) Ilhan, F.; Galow, T. H.; Gray, M.; Clavier, G.; Rotello, V. M. *J. Am. Chem. Soc.* **2000**, *122*, 5895–5896.
- (5) Kabanov, A. V.; Bronich, T. K.; Kabanov, V. A.; Yu, K.; Eisenberg, A. J. *Am. Chem. Soc.* **1998**, *120*, 9941–9942.

- (6) Boal, A. K.; Ilhan, F.; DeRouchey, J. E.; Thurn-Albrecht, T.; Russell, T. P.; Rotello, V. M. *Nature* **2000**, *404*, 746–748.
- (7) Frankamp, B. L.; Uzun, O.; Ilhan, F.; Boal, A. K.; Rotello, V. M. *J. Am. Chem. Soc.* **2002**, *124*, 892–893.
- (8) Dinsmore, A. D.; Hsu, M. F.; Nikolaidis, M. G.; Marquez, M.; Bausch, A. R.; Weitz, D. A. *Science* **2002**, *298*, 1006–1009.
- (9) Wong, M. S.; Cha, J. N.; Choi, K.; Deming, T. J.; Stucky, G. D. *Nano Lett.* **2002**, *2*, 583–587.

Materials and Methods

Homopolymer Polyelectrolytes. Poly-L-lysine₁₀₀, poly-L-lysine₂₀₀, and poly-L-lysine₃₀₀ were synthesized from *N*_ε-carboxybenzyl-L-lysine *N*-carboxyanhydrides and the initiator 2,2'-bipyridyl-Ni(1,5-cyclooctadiene)¹⁰ with polydispersities ranging from 1.05 to 1.4. The CBZ-L-lysine polymers were then deprotected (to give the free amine functional group) using a mixture of trifluoroacetic and 33% hydrobromic acid in glacial acetic acid; the excess acid was later removed by dialysis. Commercial poly-L-lysine (molecular weight range 25 000–60 000), poly-L-arginine (molecular weight range 15 000–70 000), and polyallylamine (molecular weight ≈ 70 000) were purchased from Sigma-Aldrich.

Citrate-Stabilized CdSe/CdS Core–Shell QDs. Water-soluble, citrate-stabilized QDs were synthesized as previously reported by Rogach et al.¹¹ Two final sets of QDs corresponding to green and orange-red emission were used for the vesicle assembly. The as-synthesized core–shell QDs were characterized by TEM, UV–vis absorbance, and fluorescence measurements. The results of these characterizations agreed with the data presented by Rogach et al.¹¹

Thioglycolic Acid Solubilized TOPO-Stabilized CdSe QDs. Trioctylphosphine oxide (TOPO)-stabilized CdSe QDs were synthesized and rendered water-soluble through ligand exchange with thioglycolic acid as reported by Chan and Nie.¹²

Quantum Dot Vesicle Assembly. The polyelectrolytes, regardless of molecular weight, were dissolved in deionized water at concentrations of 5 mg/mL. 100 μL of the as-synthesized QD solution was first diluted to 200 μL total volume with deionized water. The 200 μL QD aliquot was then added to 50 μL of the polyelectrolyte solution, whereafter the solution turned cloudy. The reaction was vigorously mixed by manual pipetting, during which the solution altered in turbidity from the initial cloudy suspension to a macroscopically clearer solution. The vesicles were imaged using both bright field and fluorescence optical microscopy; the fluorescence images were done using a continuous wave argon ion 365 nm laser line.

Dynamic Light Scattering Measurements of the Nanoparticle Vesicles. All nanoparticle vesicles were prepared immediately prior to measurements. Dynamic light scattering measurements were made on a Brookhaven Instruments BI-9000AT Digital Correlator as a function of scattering angle (30–150°) at room temperature with sampling delay times from 1 μs to 10 s. The raw data were analyzed by least-squares fits to a cumulant expansion to which two additional long decays were added: $a_0 + a_1 \exp(-2k_1\tau + k_2\tau^2 - (1/3)k_3\tau^3) + a_2 \exp(-2k_{21}\tau) + a_3 \exp(-2k_{31}\tau)$. The two long decay rate monoexponential functions were included to model very large assemblies, probably arising from conglomerates of spherical assemblies and/or the presence of dust. The hydrodynamic radius, R_H , of the spheres was extracted by fitting the Stokes expression to the decay rate constants: $\Gamma = k_1 = q^2D = q^2Tk_B/6\pi\eta R_H$.

The dependence of QD vesicle size on polymer chain length was studied through DLS measurements made on an ALV DLS-SLS 5000 system as a function of scattering angle (30–150°). The samples were again prepared immediately prior to measurements and were made such that the molar concentrations of polymer chains and QDs were kept constant throughout and that the only changing variable was the number of repeat units per polypeptide chain.

Nanoparticle Hollow Sphere Synthesis. The silica QD hollow spheres were generated by adding 200 μL of the commercially available colloidal silica, Snowtex 0 (10–20 nm particle size, Nissan Chemical), to the preformed QD vesicle solutions. The hollow spheres were allowed to settle to the bottom of the tubes before characterization by optical and electron (SEM and TEM) microscopy.

Scanning and Transmission Electron Microscopy. Scanning electron microscopy (SEM) images were taken on a JEOL 6340F field emission gun microscope, and the transmission electron microscopy (TEM) was done on a JEOL 2000FX analytical microscope.

Confocal Microscopy. Laser scanning confocal microscopy was performed using a Zeiss 510 microscope equipped with an ArKr laser using 488 nm light to excite the QDs. A droplet of the nanoparticle hollow sphere solution was sandwiched between a glass slide and a coverslip. The solution used for this experiment was prepared from 50 μL of poly-L-lysine₂₀₀ solution, 125 μL of CdSe/CdS QD solution, and 125 μL of Snowtex 0 solution.

Results and Discussion

The addition of citrate-stabilized core–shell QDs to the poly-L-lysine solutions caused the initial transparent polymer mixtures to become visibly turbid and cloudy, indicating aggregation of the positively charged polypeptide with the negatively charged QDs. Upon continued mixing, the solutions changed from cloudy to clear, and light microscopy imaging revealed what looked like oil droplets in an aqueous medium (Figure 1). Fluorescence microscopy, using the QDs as emitting species, revealed that the QDs are concentrated in/on the droplets, Figure 1b. Dynamic light scattering measurements gave effective diameters similar to those seen by optical microscopy. When comparing the samples prepared by poly-L-lysine₁₀₀, poly-L-lysine₂₀₀, and poly-L-lysine₃₀₀ by DLS, we found that the effective diameter of the as-synthesized vesicles appeared to increase almost linearly (from 0.85 to 1.67 μm) with the length of the polypeptide. However, there was very little difference in vesicle dimension between those made using the 300- and 400mer polymers.

While the as-assembled QD nanoparticle vesicles collapsed upon air-drying, the addition of silica nanoparticles to the reaction media, after the introduction of QDs, produced stable three-dimensional hollow spheres with distinct compositional siting of the two types of nanoparticles. Laser scanning confocal microscopy of the hollow spheres clearly showed the three-dimensional, hollow nature of the final structures (Figure 2A). The shell walls of these hollow spheres are formed of a distinct inner layer of QDs followed by a thinner outer layer of silica nanoparticles (Figure 2B). Similar QD hollow spheres produced using specifically tailored diblock copolypeptides have been shown to provide single mode quantum dot microcavity lasing.¹³

The formation of these QD vesicles was found to be stringently dependent on the overall molar charge ratios of the negative citrate molecules to the positive amines of poly-L-lysine. The allowed window was narrow and determined to be between 0.30 and 0.40 (negative citrate charges to positive amine charges). At ratios below 0.3, the addition of citrate-stabilized QDs leads to neither cloudiness nor vesicles, and at ratios above 0.4, the solutions initially turned cloudy followed by a rapid precipitation of both nanoparticles and polymer. At high ratios of QDs to polymer, the substantial charge matching between the negative citrate and positive amine groups presumably causes insolubility.

To further understand the molecular chemistry occurring at the interface between the nanoparticles and the polyelectrolyte, QDs with other negatively charged stabilizing ligands were synthesized and reacted with the cationic polyelectrolytes.

(10) Deming, T. J. *Nature* **1997**, *390*, 386–390.

(11) Rogach, A. L.; Nagesha, D.; Ostrander, J. W.; Giersig, M.; Kotov, N. A. *Chem. Mater.* **2000**, *12*, 2676–2685.

(12) Chan, W. C. W.; Nie, S. M. *Science* **1998**, *281*, 2016–2018.

(13) Cha, J. N.; Bartl, M. H.; Wong, M. S.; Popitsch, A.; Deming, T. J.; Stucky, G. D. *Nano Lett.* **2003**, ASAP Article.

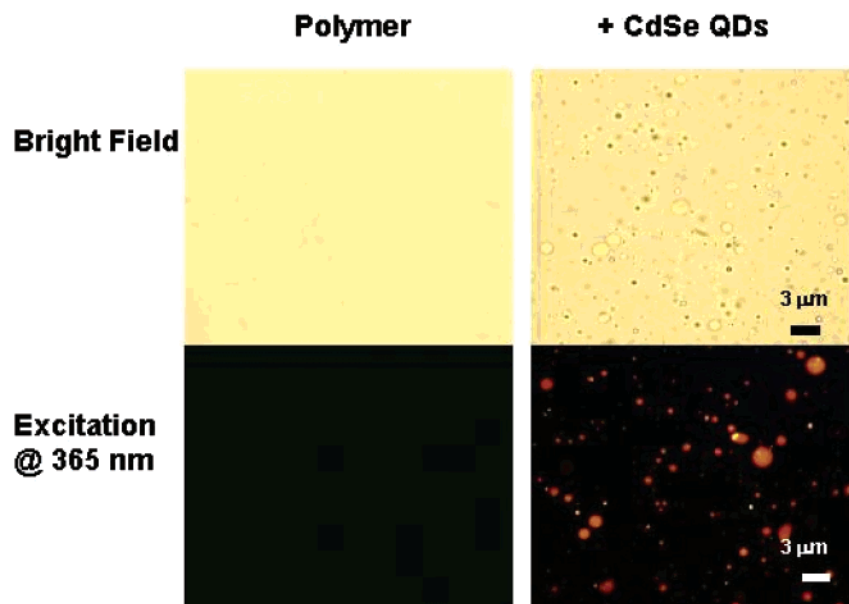


Figure 1. Bright field and fluorescence optical microscopy images of polymer solutions before and after the addition of poly-L-lysine₂₀₀ to the citrate-stabilized CdSe/CdS core-shell QDs at a ratio of 0.375 carboxylate to amine charges. The fluorescence images were obtained using the 365 nm line of a continuous wave argon ion laser. While the polyelectrolyte solutions demonstrated no visible macroscopic phase separation, the addition of the negatively charged QDs caused an oil-in-water-like emulsion to form. The size of these droplets visibly varied from approximately 1 to 3 μm , and these values roughly correlated to the effective diameters determined from dynamic light scattering measurements.

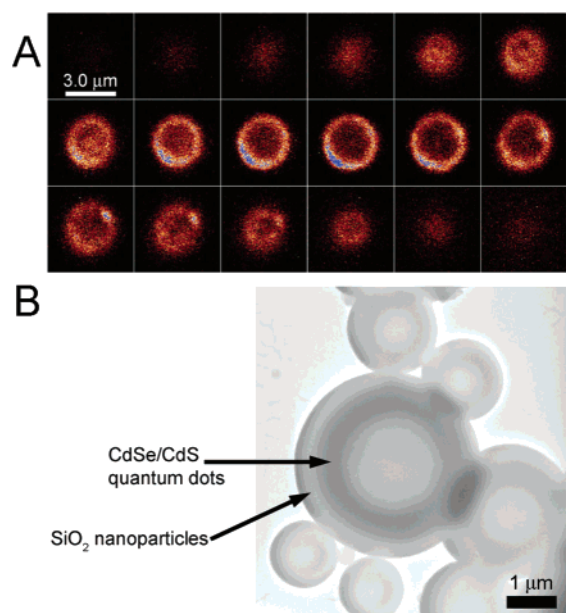
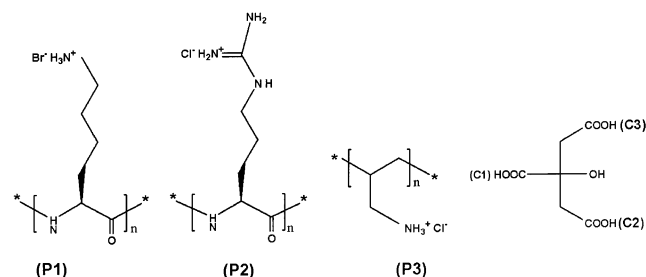


Figure 2. (A) Laser scanning confocal image of a single nanoparticle hollow sphere. The cross-sectional pictures are shown in series from the top of the sphere (top left image) to the bottom (bottom right image), clearly depicting the three-dimensional, hollow nature of the final structure. The imaged hollow sphere is about 3.2 μm in diameter. (B) Transmission electron micrograph of a self-assembled hollow sphere where the cavity wall is composed of a close-packed inner layer of core-shell CdSe/CdS citrate-stabilized QDs followed by a distinct outer layer of silica nanoparticles.

Trioctylphosphine (TOPO)-stabilized CdSe QDs made water-soluble by ligand exchange with thioglycolic acid¹² were mixed with solutions of poly-L-lysine or polyallylamine (for a discussion of polyallylamine in the assembly process, see below), but, unlike the results obtained using the citrate-functionalized QDs, no vesicles or any other observable supramolecular organization was detected. This result demonstrates that simply using negatively charged, carboxylic acid-functionalized nanoparticles

Chart 1. The Chemical Structures of the Polyamine-Based Polyelectrolytes Used in the Reactions^a



^a (P1) Poly-L-lysine hydrobromide. (P2) Poly-L-arginine hydrochloride. (P3) Polyallylamine hydrochloride. The chemical structure of citric acid with the carboxylic acid denoted from lowest to highest $\text{p}K_{\text{a}}$: C1 with a reported $\text{p}K_{\text{a}}$ of 3.128, C2 with a reported $\text{p}K_{\text{a}}$ of 4.761, and C3 with a reported $\text{p}K_{\text{a}}$ of 6.396.²¹

is not sufficient to drive phase separation and assemble the QDs into vesicles. The initial part of the synthesis of the citrate-stabilized CdSe nanoparticles involves the complexation of free Cd^{2+} ions with citrate molecules in water at pH 9.0. From the three relative $\text{p}K_{\text{a}}$'s of citric acid, it can be deduced that the Cd^{2+} ions are binding the carboxylic acid groups with the two lowest $\text{p}K_{\text{a}}$'s, specifically 3.1 ($\text{p}K_{\text{a}}$) (Chart 1, C1) and 4.8 ($\text{p}K_{\text{a}}$) (Chart 1, C2). This binding scheme is in accordance with the observed behavior of Al(III), Ga(III),¹⁴ and Zn(II)¹⁵ in crystal structures. The final QDs are then structured such that the only surface accessible carboxylic acid group is that corresponding to the most basic $\text{p}K_{\text{a}}$ of 6.4 ($\text{p}K_{\text{a}}$) (Chart 1, C3), and, hence, it must be this specific functionality that interacts with the primary amine of poly-L-lysine.

To substantiate this theory, we investigated the influence of pH on the QD vesicle assembly. As demonstrated in Table 1,

- (14) Matzapetakis, M.; Kourgiantakis, M.; Dakanali, M.; Raptopoulou, C. P.; Terzis, A.; Lakatos, A.; Kiss, T.; Banvai, I.; Iordanidis, L.; Mavromoustakos, T.; Salifoglou, A. *Inorg. Chem.* **2001**, *40*, 1734–1744.
 (15) Swanson, R.; Ilsley, W. H.; Stanislawski, A. G. *J. Inorg. Biochem.* **1983**, *18*, 187–194.

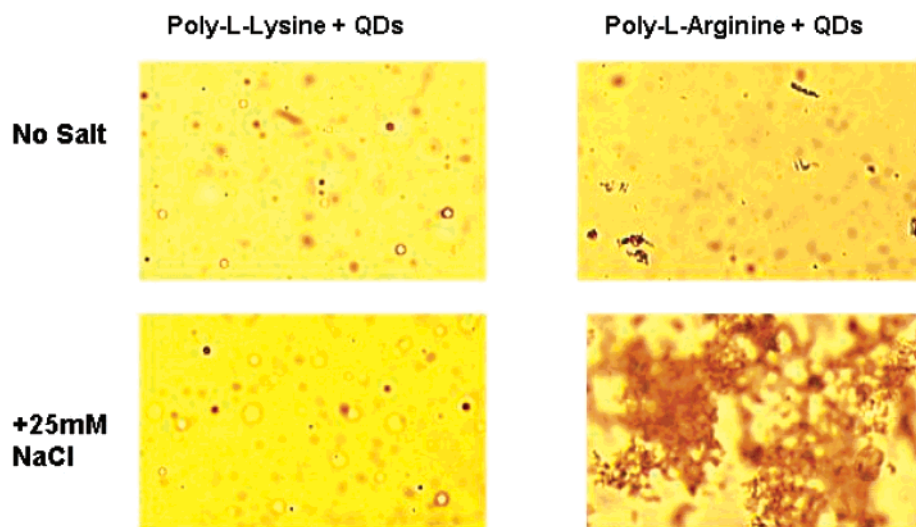


Figure 3. Bright field optical microscopy images revealing the effect of the addition of sodium chloride (25 mM NaCl) to the reaction mixtures. While the poly-L-lysine₂₀₀ QD vesicles remained macroscopically intact up to at least 40 mM NaCl, the addition of as little as 2 mM NaCl caused rapid and massive flocculation in the poly-L-arginine reactions.

Table 1. Data Detailing the Effect of pH on the Synthesis of the QD Vesicles from Poly-L-lysine₂₀₀ and Citrate-Stabilized CdSe/CdS Core–Shell QDs at a Ratio of 0.375 Carboxylate to Amine Charges

pH of citrate-capped QD solution	pH of poly-L-lysine solution	vesicle formation?
5.0	7.0	no
5.5	7.0	no
6.0	7.0	no
6.5	7.0	yes
7.0	7.0	yes
8.0	7.0	yes
9.0	7.0	yes
9.5	7.0	yes
7.0	12.0	no

the spontaneous formation of the nanoparticle vesicles appeared to depend on both the pK_3 of citric acid (6.4) as well as the pK_a of poly-L-lysine (10.5). At pH values below 6.5 and above 11, the spontaneous formation of vesicles was prohibited, and, furthermore, no initial cloudiness or turbidity was detected during any stage of the reactions. Furthermore, the synthesized QD vesicles were found to be sensitive to pH: when the pH of the vesicle solutions was changed to either below 6 or above 11, the assembled structures were destroyed. This observation is of particular interest with respect to the possible use of the vesicles as pH-controlled transport vehicles. These pH experiments demonstrate that the supramolecular assembly of the vesicles is charge dependent because both the neutralization of the citrate carboxylic acid ($pH < 6.5$) and the amine of poly-L-lysine ($pH > 10.5$) hindered the assembly process. Furthermore, the negative result obtained at pH 6.0 provides strong evidence that the molecular interaction between the QDs and the polyelectrolyte is dependent on the C3 (Chart 1) carboxylic acid of citric acid.

We also tried a different cationic polypeptide, poly-L-arginine ($pK_a \approx 12.5$, P2 in Chart 1), as a reagent with the citrate-stabilized QDs. Surprisingly, using polymer chain length dimensions and working concentrations similar to those employed for poly-L-lysine, we found that the addition of citrate-stabilized QDs only caused the poly-L-arginine solutions to become turbid with no ensuing phase transition into vesicles.

Electron microscopy of the final products showed no vesicular geometries and only coagulated materials. However, the non-amino-acid-based polyamine, polyallylamine, with its corresponding pK_a of ~ 10.5 (Chart 1, P3), spontaneously produced nanoparticle vesicles when mixed with the citrate-functionalized CdSe QDs. One possible explanation of the striking differences observed in the products obtained between poly-L-lysine and poly-L-arginine is that the higher pK_a of poly-L-arginine ($pK_a \approx 12.5$) leads to weaker hydrogen bonding (see below).

The assembly process and the responsiveness and stability of the assemblies were further investigated by adding salt (NaCl) to a solution of the QD vesicles. It has previously been shown that the addition of salt to polyelectrolyte complexes (PECs) causes substantial flocculation of the PECs.^{16,17} As demonstrated in Figure 3, while final working concentrations of 2–50 mM NaCl induced drastic changes in the poly-L-arginine nanoparticle reactions with substantial flocculation of QDs and polymer, the addition of salt caused little or no qualitative change in the poly-L-lysine reactions. Furthermore, microscopy analyses of the lysine systems revealed that the assembled QD vesicles became smaller upon addition of salt and remained intact up to a final NaCl concentration of at least 40 mM. Preliminary light scattering data indicate that the vesicles remain intact to a NaCl concentration of 250 mM. The flocculation observed in the poly-L-arginine reaction mixtures provides strong evidence that the molecular interactions in the poly-L-arginine/QD complexes are similar to that of the traditional organic PECs and are predominantly electrostatic. However, in the poly-L-lysine system, the stability of the nanoparticle vesicles to salt substantiates the hypothesis that the ligands on the nanoparticles and the polymer are interacting through charge-stabilized hydrogen bonding.

On the basis of the visible and microscopic observations, pH titration, and salt gradient experiments, a model can be proposed for the interfacial molecular forces that drive the macroscopic phase separation and formation of the poly-L-lysine nanoparticle vesicles (Figure 4). When the negatively charged citrate-

(16) Buchhammer, H.-M.; Petzold, G.; Lunkwitz, K. *Langmuir* **1999**, *15*, 4306–4310.

(17) Dautzenberg, H.; Karibyants, N. *Macromol. Chem. Phys.* **1999**, *200*, 118–125.

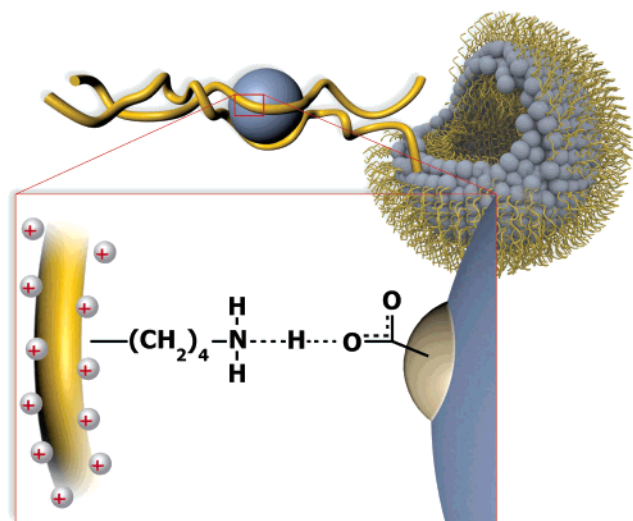


Figure 4. A schematic diagram of the nanoparticle vesicles and the directional charge-stabilized hydrogen bonds that form between the amines of the poly-L-lysine and the carboxylic acid group (pK_3) of the citrate-stabilized QDs. The quantum dots form the “oily” zone and what extends into the exterior and interior water regions are the portions of the poly-L-lysine chains that are not coordinated with the carboxylic acid groups of the citrate-stabilized nanoparticles.

stabilized QDs are first introduced into the poly-L-lysine solutions, the transparent polymer solutions become turbid, indicating aggregation due to long-range Coulombic attractive forces and charge matching. The initial cloudy solutions then undergo a phase change to an oil-in-water-like emulsion (Figure 1), and it is proposed that this is due to a transition in the interfacial molecular forces from pure electrostatic charge–charge interactions to directional charge-stabilized hydrogen bonding (Figure 4). Hydrogen bonds are expected to be strongest when the difference in pK_a between the donor and acceptor is small.^{18–20} The substantial difference of 6 pK_a units between the primary amine of poly-L-arginine and the carboxylic acid group (Chart 1, C3) of citric acid may explain why polyallylamine ($pK_a \approx 10.5$) and poly-L-lysine ($pK_a \approx 10.5$), which have a smaller difference of ~ 4 pK_a units, could successfully assemble the citrate-stabilized QDs into vesicles, while poly-L-arginine could not. However, it is also possible that the bulkiness and charge delocalization of the arginine side chain play additional inhibiting roles.

Conclusions

We propose that the combination of electrostatic affinities and hydrogen bonding between the poly-L-lysine and the citric

acid-functionalized QDs creates a zone of water exclusion around each nanoparticle where the water molecules originally solvating the charged ligands are driven to the bulk phase of water. This provides an entropy increase that further lowers the assembly free energy. As stated earlier, an excess number of positive charges associated with the polymer relative to the number of carboxylic acid groups (pK_3) is required for these vesicles to form, and it is therefore safe to assume that the initially negatively charged pK_3 carboxylic acid group of the citrate-coated QDs is effectively neutralized after reaction with the polypeptide. These screened QDs in essence then become what is typically the lipid layer of a conventional organic vesicle, and the excess poly-L-lysine chains that are not interacting with any nanoparticle become what are usually the polar headgroups (Figure 4).

One predominant noncovalent interaction used in biological systems is that of directional, charge-stabilized hydrogen bonding, where the strength of these interactions is dependent on the relative pK_a values of the donor and acceptor groups. The model that we propose here is an adaptation of this noncovalent chemistry for the supramolecular assembly of semiconductor nanoparticles into vesicles starting from completely charged species. While one of the more common bioinspired techniques for producing nanoparticle superstructures has been to use entire biomolecules and molecular recognition, we have provided here an alternative, simpler, more generalized, and possibly versatile approach for the multicompositional, three-dimensional cooperative assembly of organic and inorganic species into spatially defined domains.

Acknowledgment. We thank Dr. Michael Wyrsta for assistance and helpful discussions. We thank Matthew Hirschev for assistance with the confocal microscopy measurements. We thank Peter Allen (Department of Computer Science and Engineering, UCSB) for the artful rendering of the nanoparticle vesicles (Figure 4). We also thank Tim Rapp (UC Berkeley) for assistance with DLS measurements. We gratefully acknowledge the financial support of NASA-JPL and the Danish Natural Sciences Research Council (H.B.). This material is based upon work supported in part by the National Science Foundation under Grant No. DMR 9634396. This work made use of MRL Central Facilities supported by the National Science Foundation under Award No. DMR00-80034.

Note Added after ASAP Publication: The version published on the Web 6/13/2003 contained errors in Chart 1. The final Web version published 6/17/2003 and the print version are correct.

- (18) Goerbitz, C. H. *Acta Crystallogr., Sect. B* **1989**, *45*, 390–395.
 (19) Overgaard, J.; Schiott, B.; Larsen, F. K.; Iversen, B. B. *Chem.-Eur. J.* **2001**, *7*, 3756–3767.
 (20) Gilli, P.; Bertolasi, V.; Ferretti, V.; Gilli, G. *J. Am. Chem. Soc.* **1994**, *116*, 909–915.
 (21) Bates, R. G.; Pinching, G. D. *J. Am. Chem. Soc.* **1949**, *71*, 1274–1283.

JA0279601